HHS Public Access

Author manuscript

Chemosphere. Author manuscript; available in PMC 2022 June 01.

Published in final edited form as:

Chemosphere. 2021 June ; 273: 129607. doi:10.1016/j.chemosphere.2021.129607.

Intestinal changes associated with fluoride exposure in rats: Integrative morphological, proteomic and microbiome analyses

Aline Dionizio[1], **Dawud Abduweli Uyghurturk**[2], **Carina Guimarães Souza Melo**[1], **Isabela Tomazini Sabino-Arias**[1], **Tamara Teodoro Araujo**[1], **Talita Mendes Silva Ventura**[1], **Juliana Vanessa Colombo Martins Perles**[3], **Jacqueline Nelisis Zanoni**[3], **Pamela Den Besten**[2,*], **Marília Afonso Rabelo Buzalaf**[1,*]

[1]Department of Biological Sciences, Bauru School of Dentistry, University of São Paulo, Bauru, Brazil

[2]Department of Orofacial Sciences, School of Dentistry, University of California, San Francisco, San Francisco, USA

[3]Department of Morphophysiological Sciences, State University of Maringá, Maringá, Brazil

Abstract

Gastrointestinal signs and symptoms are the first signs of toxicity due to exposure to fluoride (F). This suggests the possibility that lower levels of subchronic F exposure may affect the gut. The aim of this study was to evaluate changes in the morphology, proteome and microbiome of the ileum of rats, after subchronic exposure to F. Male rats ingested water with 0, 10, or 50 mgF/L for thirty days. Treatment with F, regardless of the dose, significantly decreased the density of HuC/D-

[*]**Corresponding authors** Marília Afonso Rabelo Buzalaf- Department of Biological Sciences, Bauru School of Dentistry, University of São Paulo, Bauru, Brazil; mbuzalaf@fob.usp.br; Pamela Den Besten- Department of Orofacial Sciences, School of Dentistry, University of California, San Francisco, San Francisco, California, USA; pamela.denbesten@ucsf.edu.

Author Contributions

C.M., M.B., J.Z., A.D and J.P. conceived the experiments. A.D. and C.M. conducted the experiments. A.D., C.M., T.A, J.P., I.A., T.V., J.Z and A.U. participated in the research experiments. A.D., C.M., A.U, P.B, M.B participated in the experiments analysis. A.D., C.M., P.B, M.B. drafted the article; analyzed and interpreted the results. All authors reviewed and approved the manuscript.

Aline Dionizio (A.D)
Dawud Abduweli Uyghurturk (A.U)
Carina Guimarães Souza Melo (C.M)
Isabela Tomazini Sabino-Arias (I.A)
Tamara Teodoro Araujo (T.A)
Talita Mendes Silva Ventura (T.V)
Juliana Vanessa Colombo Martins Perles (J.P)
Jacqueline Nelisis Zanoni (J.Z)
Pamela Den Besten (P.B)
Marília Afonso Rabelo Buzalaf (M.B)

Conflict of interest statement

The authors have declared no conflict of interest.

Additional Information

Supplementary information accompanies this paper.

Declaration of interests

☒ The authors declare that they have no known competing financial interests or personal relationships that could have appeared to influence the work reported in this paper.

IR neurons, whereas CGRP-IR and SP-IR varicosities were significantly increased compared to the control group. Increased VIP-IR varicosities were significantly increased only in the group treated with 50 mgF/L. A significant increase in thickness of the tunica muscularis, as well as in the total thickness of the ileum wall was observed at both F doses when compared to controls. In proteomics analysis, myosin isoforms were increased, and *Gastrotopin* was decreased in F-exposed mice. In the microbiome metagenomics analysis, Class Clostridia was significantly reduced upon exposure to 10 mgF/L. At the higher F dose of 50 mg/L, Genus Ureaplasma was significantly reduced in comparison with controls. Morphological and proteomics alterations induced by F were marked by changes associated with inflammation, and alterations in the gut microbiome. Further studies are needed to determine whether F exposure increases inflammation with secondary effects of the gut microbiome, and/or whether primary effects of F on the gut microbiome enhance changes associated with inflammation.

Graphical Abstract

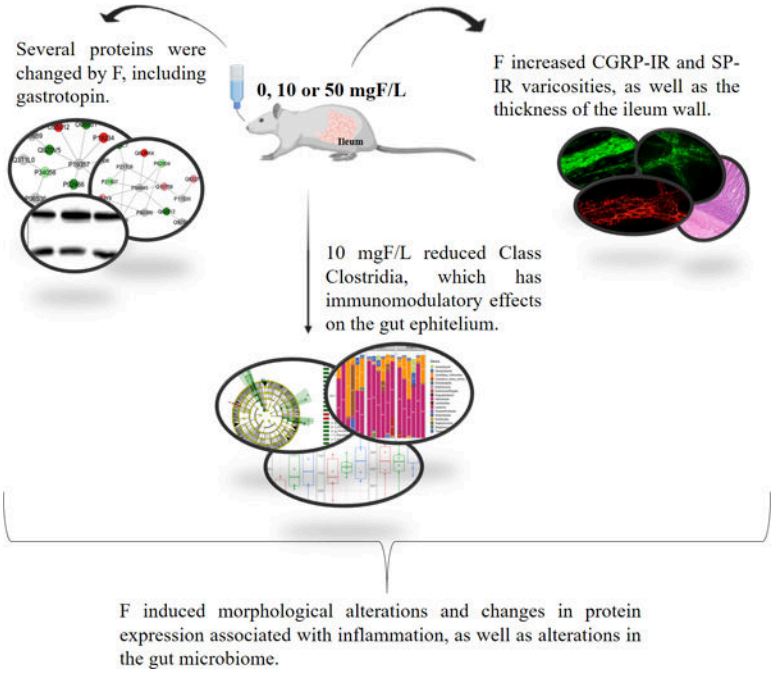

Keywords

Fluoride; gastrointestinal symptoms; microbiome; Crohn’s disease; ileum

INTRODUCTION

Since the second half of the last century fluorides have been largely used to control dental caries (ten Cate and Buzalaf, 2019) but excessive intake may cause side-effects, among which dental fluorosis is the most commonly observed (Iheozor-Ejiofor et al., 2015). Exposure to higher doses of fluoride (F) has been shown to interfere in several biochemical pathways such as redox balance, signal transduction and apoptosis (Strunecka et al., 2007; Barbier et al., 2010; Wei et al., 2018; Zuo et al., 2018).

It is known that approximately 25% of the F ingested is absorbed in the stomach in the form of hydrofluoric acid, in a pH-dependent manner (Whitford and Pashley, 1984), and the remaining, approximately 75%, is absorbed in the ionic form (F^{-}) in the small intestine, in a process independent of the pH (Nopakun et al., 1989; Nopakun and Messer, 1990). The gastrointestinal tract (GIT) is the main route of exposure to F (Zheng et al., 2002), with gastrointestinal signs and symptoms like vomiting, abdominal pain, nausea and diarrhea being the initial signs of F toxicity (Susheela, 1992; Susheela et al., 1993; Das et al., 1994; Sharma, 2009).

Recently, we found proteomic and morphological alterations in the duodenum (Melo et al., 2017) and jejunum (Dionizio et al., 2018b) of rats with subchronic exposure to F from the drinking water, as well as alterations in the morphology of different types on enteric neurons (Melo et al., 2017; Dionizio et al., 2018c). These alterations could help to explain the gastrointestinal symptoms classically reported in cases of toxicity induced by excess F ingestion. It should be considered that there is bidirectional communication between gut and CNS, which is known as the gut-brain axis (GBA) that integrates brain and gastrointestinal functions (Collins and Bercik, 2009). The GIT is composed of an interconnected network of neurons arranged in the walls of the gut, which controls its function, known as the Enteric Nervous System (ENS) (Furness, 2006). Changes in this system can affect the permeability, secretion, motility, and absorption of the GIT (Sand et al., 2014). Moreover, the gut microbiome, composed of bacteria, archaea, and eukaryotes colonized in the human gastrointestinal tract, with an approximate amount of human cells (Sender et al., 2016) is integrated to the GBA, constituting the so-called microbiota-gut-brain axis (MGBA). The gut microbiome has been found to be associated with the development of various diseases including obesity and types 2 diabetes (Allin et al., 2015; Tai et al., 2015), liver disease (Llorente and Schnabl, 2015), intestinal inflammatory syndromes (Goto et al., 2015; Wright et al., 2015), allergic diseases (McCoy and Koller, 2015), CNS diseases (Fond et al., 2015; Felice and O'Mahony, 2017; Bell et al., 2019), and autoimmune diseases (Johnson et al., 2015; Lerner and Matthias, 2015).

The small intestine has a lower and more diverse, but more dynamic microbial biomass that distinctly differs from that of the large intestine (Kastl et al., 2020). Although stool samples are most commonly collected in studies of the gut microbiota, stool more accurately represents the large intestine portion of the gut. The ileum has the highest microbial biomass in the small intestine, and thus, the present study morphologically evaluated the different subtypes of enteric neurons of the ileum of rats subchronically exposed to F. Proteomics methods were used to analyze the changes in the protein profile of the ileum after exposure to F, to provide mechanistic rationales, as well as to help the understanding of the possible causes of the signs and symptoms commonly described in cases of toxicity caused by this ion. Moreover, considering that excessive exposure to F might affect both the gut (Melo et al., 2017; Dionizio et al., 2018c) and the CNS (Duan et al., 2018; Goschorska et al., 2018; Strunecka and Strunecky, 2019) and the role of the microbiome in the GBA, we also investigated the effect of subchronic exposure to F through the drinking water on the microbiome of the ileum of rats.

METHODS

Treatment

The protocols used in the study were approved by the Ethics Committee for Animal Experiments of Bauru School of Dentistry, University of São Paulo (protocols 014/2011 and 012/2016). Sixty-day-old 18 adult male rats (*Rattus norvegicus*, Wistar) were housed individually in metabolic cages under controlled lighting schedule and temperature (22±2°C), with access to food and water *ad libitum*. The animals were randomly divided into 3 groups (n=6 per group), according to the F concentration (as NaF) in the drinking water that was administered for 30 days at concentrations of 0, 10, or 50 mg/L. These F concentrations correspond to ~2 and 10 mg/L in the drinking water of humans because F metabolism is 5 times faster in rodents than in humans (Dunipace et al., 1995). The ileum was harvested for immunofluorescence, histological analysis, proteomic analysis, Western blotting and 16S rRNA gene sequencing. To collect the ileum, the cecum was first localized and 2 incisions for its removal were conducted: the first in the anterior portion of the ileocecal valve (distal incision) and the second, 10 centimeters proximally the first one. Tissues for proteomic analysis and Western blotting were frozen at −80°C. The remaining tissues were fixed in 10% paraformaldehyde and processed either for histology or for microbiome analyses.

Histomorphometric and immunofluorescence analyses

The parameters evaluated in the histomorphometric analysis were thickness of the tunica muscularis and thickness of the ileum wall. In the immunofluorescence analysis, we evaluated neurons immunoreactive to: human proteins type C and D (HuC/D-IR) and neural nitric oxide synthase (nNOS-IR). The primary antibodies used were anti-HuC/D (A-21271, Invitrogen, Walthm, Massachusetts, USA), and anti-nNOS (H-299, sc-8309 Santa Cruz, Dallas, Texas, USA), respectively. We also evaluated varicosities immunoreactive to: substance P (SP-IR), intestinal vasoactive peptide (VIP-IR) and calcitonin gene-related peptide (CGRP-IR). The primary antibodies used were Anti-Substance P (sc9758, Santa Cruz, Dallas, Texas, USA), Anti-VIP (V0390, Sigma-Aldrich, St. Louis, MO), Anti-CGRP (AB15360, Millipore, St Charles, MO), respectively.

The details of the analyses are described elsewhere (Melo, Perles et al. 2017). See also supplemental data for experimental details.

Proteomic analysis

Label-free proteomic analysis was performed in a nanoACQUITY UPLC system (Waters, Milford, MA) coupled to a Xevo Q-TOF G2 mass spectrometer (Waters, Milford, MA), as described elsewhere (Lobo, Leite et al. 2015). The nanoACQUITY UPLC system is equipped with a Trap Columm (100Å, 5 μm, 180 μm × 200 mm) and a HSS T3 M-Class type column (analytical column 75 μm × 150 mm; 1.8 μm) (Waters, Milford, MA). ProteinLynx GlobalServer software (PLGS) version 3.03 (Waters, Milford, MA) was used to process and search the LC-MSE continuum data.

Peptides identification and difference in expression among the groups was obtained using the Protein Lynx Global Server (PLGS) software (version 3.03, Waters Co., UK) as described elsewhere (Lima Leite, Gualiume Vaz Madureira Lobo et al. 2014). The procedures and bioinformatics analysis were performed as described previously (Dionizio, Melo et al. 2018, Dionizio, Melo et al. 2020).

Western blotting analysis

The Western blotting was performed as previously described (Yan et al., 2012). The ileum was homogenized in lysis buffer (7 M urea, 2 M thiourea, 40 mM Dithiothreitol, all diluted in AMBIC solution), supplemented with protease inhibitors, to obtain protein extracts. Membranes were probed with commercially available *Gastrotropin* (1:500 dilution), followed by HRP-conjugated anti-rabbit antibody (1:10000) for *Gastrotropin* and *α-Actinin* (1:1000 dilution) and ECL Plus detection reagents. Relative *Gastrotropin* and *α-Actinin* band densities were obtained by densitometry as described previously (Dionizio et al., 2018a).

16S rRNA gene sequencing and bioinformatics

Total DNA was extracted using the ZR Fungal/Bacterial DNA MicroPrep ™ Kit (Zymo Research Code D6007) according to manufacturer's protocol and underwent quality analysis by fluorescence quantitation using the Qubit® 3.0 Fluorometer and QubitTM dsDNA Kit BR Assay (Thermo Fisher Scientific). The V4 region of the 16S rRNA gene was amplified using universal primers (515F: GTGCCAGCMGCCGCGGTAA and 806R: GGACTACHVGGGTWTCTAAT). These primers were tailed with sequences to incorporate Illumina adapters with indexing barcodes. The amplification program consisted of initial denaturation at 94 °C for 3 min, followed by 29 cycles of denaturation at 94 °C for 45 sec, annealing at 50 °C for 60 sec; extension at 72°C for 90 sec and a final extension at 72 °C for 10 min. Amplification reactions were conducted in Veriti ™ Thermal Cycler (Applied Biosystems). Samples were barcoded with a unique combination of forward and reverse indexes allowing for simultaneous processing of multiple samples. The PCRs were subjected to purification steps using Agencourt AMPure XP magnetic bead (Beckman Coulter. After this step, quantification by the Real-Time PCR methodology was performed using QuantStudio3 Real-Time thermal cycler (Applied Biosystems) and KAPA-KK4824 (Library Quantification Kit - Illumina/Universal) Kit, all according to the manufacturer's protocol. An equimolar DNA pool was generated by normalizing all samples to 3vnM for sequencing, which was conducted using the Illumina MiSeq Next Generation Sequencing System and MiSeq Reagent Kit. Micro V2 300 cycles - 2 × 150bp readout. The downstream bioinformatic analyses were performed with R programming language (v 3.6.3) using forward reads of the sequencing data. After reads containing more than 2 expected errors and more than 8 consecutive same nucleotide repeats were discarded, the raw sequences were truncated to 125pb, denoised, chimera filtered using the pooled method, and clustered into sequence variants using DADA2 package (v1.14.1). Taxonomy was assigned to operational taxonomic units (OTUs; 97% clustering) using the SILVA (v138) database. Phangorn package (v2.5.5) was used for phylogenetic reconstruction. For taxonomical analysis, R/Bioconductor (Vegan, PhyloSeq, and DESeq2) software packages were used.

Statistical analysis

The software GraphPad Prism version 6.0 for Windows (GraphPad software Inc., La Jolla, Ca, USA) was used for morphometric, immunofluorescence and Western blot data analyses. Data were checked for normality (Kolmogorov-Smirnov test) and homogeneity (Bartlett test) to select the appropriate test. The thickness of the tunica muscularis and thickness of the ileum wall were compared by ANOVA followed by Bonferroni's test. Densities of HuC/D-IR and nNOS-IR were compared by ANOVA followed by Fisher's test. CGRP-IR, VIP-IR and SP-IR and cell bodies areas of HuC/D-IR and nNOS-IR data compared by ANOVA followed by Tukey's test. Western blot data was compared by ANOVA, followed by Tukey's test. In all cases, the significance level was set at 5%. Data were expressed as mean ± SD.

For proteomics data, the PLGS software was used, employing Monte Carlo algorithm ($p < 0.05$ for down-regulated proteins and $1\text{-}p > 0.95$ for upregulated proteins).

In the metagenomic analyses, richness and diversity were estimated using Chao1 and Shannon estimators, respectively, as implemented in the Vegan package. Principal Coordinates Analysis (PCoA) and weighted, unweighted Unifrac distances were used for unconstrained ordination on genus proportions. A negative binomial fit and Wald test were run on every taxonomical level to assess differential abundance. P-values were adjusted using the Benjamini–Hochberg correction. Linear Discriminant Analysis (LDA) Effect Size (LEfSe) was performed using the Galaxy web application using default settings. Statistical significance was defined as $p \leq 0.05$ in both DESeq2 and LEfSe analysis.

RESULTS

Subchronic fluoride exposure increased the thickness of the ileum *tunica muscularis* and the total thickness of the ileum wall

Significant differences were observed among all the groups. Treatment with F significantly increased the thickness of the ileum *tunica muscularis*, as well as the total thickness of the ileum wall. Curiously, the low concentration of F led to the highest increase in both parameters. The mean thickness of the ileum *tunica muscularis* was 111.8±1.8, 160.8±5.0 and 135.1±3.5 μm^2 for the 0, 10 and 50 mgF/L, respectively. The corresponding figures for the mean total thickness of the ileum wall were 774.1±9.5, 1165.8 ± 10.7 and 833.6 ± 10.1 μm^2, respectively.

Subchronic fluoride exposure reduced the density of HuC/D-IR neurons but not of nNOS-IR neurons

HuC/D – IR—The general population of ileum neurons analyzed morphometrically found that the areas of the cell bodies (μm^2) of the HuC/D-IR neurons did not differ significantly among the groups ($p > 0.05$). However, in the analysis of the density of neurons (neurons/cm^2), a significant reduction was observed in both the F groups, in comparison with the control (Table 1).

nNOS –IR—In the morphometric analysis of the nitrergic neurons of the ileum, the cell body areas (μm^2) of the nNOS-IR neurons did not significantly differ among the groups ($p > 0.05$). The same was observed in the quantitative analysis (Table 1).

Subchronic fluoride exposure increased VIP-IR, CGRP-IR and SP-IR varicosities

In the morphometric analyses of VIP-IR varicosity areas (μm^2) of the ileum, a significant increase was detected in the group treated with 50 mgF/L with respect to the control group ($p<0.05$). For the CGRP-IR and SP-IR varicosities, a dose-response effect was observed, with significant increments in the areas as the F concentration increased (Table 1).

Images from the immunofluorescence analyzes are shown in the supplementary information (Figs. S1 and S2).

Subchronic fluoride exposure changes the proteomic profile of the ileum

The number of proteins identified in the control, 10 and 50 mgF/L groups were a total of 280, 276, and 285, respectively. Among them, 33, 69, and 40 proteins (Tables S1 and S2) were only identified in the control, 10 mgF/L and 50 mgF/L groups, respectively. In the quantitative analysis of the lower dose of F *vs.* control group, 16 proteins with alteration in expression were detected (Table S1). As for the comparison of the highest dose of F *vs.* control group, 28 proteins with alteration in expression were found (Table S2). The proteins with altered expression were mainly upregulated in the group treated with 10 mgF/L when compared with the control group. As for the comparison 50 mgF/L vs. control group, the proteins with altered expression were mainly downregulated in the treated group (Table S1 and S2).

Figures 1 and 2 show the subnetworks generated by ClusterMark® for the comparisons 10 mgF/L *vs.* control and 50 mgF/L *vs.* control, respectively. For the animals exposed to lower doses of F (Fig. 1), most of the proteins with changed expression interacted with *Solute carrier family 2, facilitated glucose transporter member 4* (GLUT4, P19357), (Fig. 1A), *Mitogen-activated protein kinase 3* (MAPK3, P21708), *5′-AMP-activated protein kinase catalytic subunit alpha-1* (AMPK subunit alpha-1, P54645), *5′-AMP-activated protein kinase subunit beta-1* (AMPK subunit beta-1, P80386), *Polyubiquitin*-6¨(Q63429) and *Dystrophin* (P11530) (Fig.1B).

As for the group treated with highest doses of F, the majority of the proteins with the change in expression interacted with *AMPK subunit alpha-1* (P54645), *AMPK subunit beta-1* (P80386), *Tumor necrosis factor* (P16599), *Phosphoglycerate mutase 2* (P16290), *Calciumactivated potassium channel subunit alpha-1* (Q62976) and *Dynein light chain 1, cytoplasmic* (P63170), *Polyubiquitin-6* (Q63429) (Fig. 2A) or *GLUT4* (P19357), *MAPK3* (P21708), *Dystrophin* (P11530), *Calcium/calmodulin-dependent protein kinase kinase 1* (CaM-kinase kinase 1, P97756) and *Regulating synaptic membrane exocytosis protein 1* (Q9JIR4) (Fig. 2B).

Subchronic fluoride exposure reduced *Gastrotropin*

Western blotting confirmed that *Gastrotropin* was significantly reduced upon exposure to F, in a dose-response manner, as revealed by proteomic analysis (Fig. 3).

Subchronic fluoride exposure changes the ileum microbiome

16S rRNA sequencing of our samples yielded high sequencing depth (Fig. S3), with the mean number of 151,396.8 reads per sample (range 112,262 – 176,734, SD 17,139.5) after quality control processes. Clustering was carried out at 97% identity to yield 802 distinct OTUs with a length of 125 bp. The SILVA 138 framework allowed 58.4% of the OTUs to be assigned to uniquely identifiable genus-level groups.

453 OTUs classified as bacteria left after filtering out OTUs assigned as Eukaryotes, Archaea, chloroplasts, and mitochondria. The most abundant phylum, family, and genus, across all samples at ≥ 1% abundance are displayed in Figure S4 and summarized in Table 2 that shows the most abundant top four taxa across all samples.

To address how microbial communities may differ between groups, we examined different α and β diversity measures. No alpha diversity metric showed a difference in richness or evenness of communities and no beta diversity metric showed clear clustering by community composition by principal coordinate analysis (Fig. S5). We next performed LEfSe and DESeq2 analyses to identify individual microbial taxa that differed between groups. Both LEfSe and DESeq2 were performed from phylum to species level (Fig. S6, S7, S8).

For the comparison control vs 10 mgF/L, in DESeq2 analysis 11 taxonomies were enriched, while 4 taxonomies were decreased in 10 mgF/L group. Class Clostridia significantly decreased in 10 mgF/L group when performed LEfSe analysis (Fig. 4a) and it was the only taxonomy that was also significantly different in DESeq2. LEfSe showed 7 taxonomies enriched in the 10 mgF/L group while 6 taxonomies decreased in 10 mgF/L group (Fig. 4b).

When control and 50 mgF/L groups were compared, genus Ureaplasma had only one OTU assigned to species and both OTU and genus of Ureaplasma was significantly decreased in the 50 mgF/L group in both LEfSe (Fig. 4c) and DESeq2 analysis. Two taxonomies increased while 5 taxonomies decreased in 50 mgF/L group with DESeq2. Nineteen taxonomies enriched in 50 mgF/L group while 2 taxonomies decreased with LEfSe analysis (Fig 4d).

DISCUSSION

F is mainly absorbed from the small intestine (Nopakun et al., 1989; Nopakun and Messer, 1990), and gastrointestinal symptoms are often reported in cases of excessive ingestion of F (Vogt et al., 1982; Augenstein et al., 1991; Gessner et al., 1994; Akiniwa, 1997). Fluoride ingestion as the result of application of a 3.5% topical F gel results in mucosal injury to the gastric epithelium in humans (Spak et al., 1990), and in previous studies of the effects of subchronic F exposure in rats, we found F related changes in the duodenum (Melo et al., 2017) and jejunum (Dionizio et al., 2018c), consistent with signs of inflammation. The present study focuses on the ileum since different segments of the small intestine have

different histological, anatomical, physiological, and functional characteristics (Guyton and Hall, 2015). Moreover, in the present study, we also evaluated the changes in the ileum microbiome upon exposure to F.

The bacterial population of the small intestine is uniquely different from that of the large intestine, owing to a more rapid transit time, the influx of digestive enzymes and bile, and intermittent food substrate delivery. The bacterial populations in the small intestine are less diverse, but more reactive, and are highest in the ileum, as it is the longest division of the small intestine where transit slows (Kastl et al., 2020). We found significant changes in bacterial populations from F exposed ileum as compared to controls. These results differed from those of Yasuda et al. (2017), who compared stool derived microbes, in mice given either 0 or 4 mgF/L in drinking water. While they found F related changes in the oral microbiome, they did not find similar changes in the gut microbiome (Yasuda et al., 2017). These differences may be due to different F exposures in the large and small intestine. As pointed out by Yasuda and colleagues, after F is largely absorbed from the small intestine, the relatively low levels of F remaining in the large intestine may not be sufficient to affect its microbiome.

In our metagenomic analyses, we found that Class Clostridia was significantly reduced upon exposure to 10 mgF/L, and Genus Ureaplasma was significantly reduced following subchronic exposure to 50 mgF/L F. It is interesting that the changes in the gut microbiome in response to F were not dose dependent. The reasons for this are not clear. However, at high F levels, certain bacteria, including Clostridia can utilize a F switch to protect themselves from the toxic effects of this ion (Baker et al., 2012). It may be that the presence of such a F switch is the reason for differential effects of F at higher as compared to lower levels of F exposure.

Clostridia are essential for the metabolic welfare of colonocytes, due to the release of butyrate as an end-product of fermentation (Pryde et al., 2002). Besides being an essential fuel to colonocytes, butyrate also promotes hyperacetylation of chromatin, by inhibiting histone deacetylases, thus influencing gene expression (Csordas, 1996). In addition, butyrate also inhibits the activation of NF-kB, decreasing the expression of proinflammatory cytokines and to anti-inflammatory effect (Segain et al., 2000; Luhrs et al., 2001). Thus, the reduction in Clostridia upon exposure to F might lead to a reduction in butyrate, with a consequent increase in inflammation. Moreover, proinflammatory cytokines are key factors in the pathogenesis of Crohn’s disease (CD), a subchronic inflammatory disorder that affects the distinct segments of the gastrointestinal tract, especially the terminal region of the ileum and the ileocecal region (Ooi et al., 2016) and in some cases can result in significant morbidity and disability (Aniwan et al., 2017).

The etiology of CD is still unknown but is probably attributed to a response to environmental agents (infection, drugs or other agents) in genetically prone individuals (Ardizzone and Bianchi Porro, 2002). In CD there is infiltration of inflammatory and immune cells (such as mast cells, macrophages, T-lymphocytes and neutrophils) that interact and release cytokines and enzymes (Aniwan et al., 2017; Gajendran et al., 2017). Activation of NF-kB, which is involved in gene transcription of proinflammatory cytokines, is increased in the intestinal

mucosa of CD patients (Segain et al., 2000). Furthermore, the gut microbiota in patients with CD has reduced butyrate-synthetic capacity (Laserna-Mendieta et al., 2018). Therefore, it may be possible that F exposure could further aggravate inflammatory conditions such as those found in CD.

We found similar effects of F as those associated with CD, including the increase in thickness of the ileum *tunica muscularis*, as well as of the total thickness of the ileum wall upon exposure to both F concentrations (Worlicek et al., 1987; Chiorean et al., 2014; Kang et al., 2017; Rosenbaum et al., 2017). These findings are consistent with increased myosin proteins observed both for 10 and 50 mgF/L (Tables S1 and S2), as myosin has been reported as possibly related to the increased thickness of the ileum *tunica muscularis*, as well as the total thickness of the ileum wall (Chu et al., 2013; Soares et al., 2015; Melo et al., 2017). The total thickness of the jejunum was also decreased upon exposure to the highest F concentration, but no alteration was found in the duodenum (Melo et al., 2017; Dionizio et al., 2018c). This increased effect of F in increasing the ileum wall may be due to a longer time of exposure in the ileum or reflect a compound cellular and microbiome effect of F in the ileum.

CD is characterized by increased intestinal permeability, associated with increase permeability of ileum epithelial cell tight junctions (Soderholm et al., 2002). Electrophysiology of epithelial cells exposed to millimolar levels of F, such as those contained in drinking water of the rats in this study, have been shown to have reduced tight junction (TJ) formation (Racz et al., 2017). Such a F related disruption of TJ formation could alter the intestinal TJ barrier, since it would result in a perturbation of the mucosal immune system and inflammation, which can act as a trigger for the development of intestinal and systemic diseases (Lee, 2015; Chelakkot et al., 2018). We found a decrease in *Calmodulin-2* in the F treated groups, which was exclusively identified in the control group. Calcium binds to calmodulin and this activates myosin light chain kinase in muscle (Guyton and Hall, 2015). Myosin light chain kinase is an important regulator of tight junction formation (Shen et al., 2006). F is known to strongly bind calcium, so perhaps a decrease in available ionic calcium may result in reduced activation of myosin light chain kinase with a potential effect on TJ formation.

Other similarities in F related effects on the ileum and those found in CD include an increase in the SP-IR varicosity area upon exposure to F, which was also observed for duodenum (Melo et al., 2017) and jejunum (Dionizio et al., 2018c). SP-IR are intense in the epithelium, cells lining the mucosal fissure, granulomas and in the muscle layers of the colon of patients with CD (Mazumdar and Das, 1992), with an increase in SP receptors in enteric neurons of the small and large intestine of CD patients, in comparison with controls and patients with ulcerative colitis (UC) (Mantyh et al., 1995).

Increases in SP are found in the serum of patients with CD (Tavano (Tavano et al., 2012) et al. 2012). SP has several effects in the CNS and in the periphery, among which are proinflammatory and strong nociceptive properties (Lembeck, 1988). SP acts in direct and indirect manners on immune cascades and on the vasculature to cause plasma extravasation, edema, and pain (Mantyh, 1991). It also stimulates intestinal smooth muscle contraction

(Holzer and Lippe, 1984), which might be implicated in the increase in the thickness of the *tunica muscularis* of the ileum, observed in the present study.

We found an increase in CGRP-IR varicosities upon treatment with F, which was also found for the duodenum, but only for the lower F concentration (Melo et al., 2017). Moreover, neurogenic inflammation that is found in CD, is also mediated by substance P and CGRP (Makharia, 2011; Munster et al., 2015). In addition to increasing in SP-IR and CGRP varicosity areas upon exposure to F, increase in VIP-IR varicosity area was also observed in the ileum of the animals treated with 50 mgF/L, as observed in our previous studies in the duodenum (Melo et al., 2017; Dionizio et al., 2018b). Increase the density of VIPergic neurons in the submucosal plexus of inflamed regions has also been reported in pediatric patients with CD (Boyer et al., 2007).

Upon exposure to F, in comparison with control, proteomic analysis showed that that many proteins with altered levels of synthesis interact with *Polyubiquitin-6* (Q63429). Polyubiquitin chains, when attached to a target protein, have different functions depending on the Lys residue of the ubiquitin that is linked. When linked to Lys-63, they are involved in DNA-damage responses as well as in signaling processes leading to activation of the transcription factor NF-kB (UNIPROT), a key mediator of inflammatory responses that induces the expression of several pro-inflammatory genes (Liu et al., 2017). In vitro and in vivo studies have shown that F upregulates NF-kB gene expression (Waugh, 2019).

Our proteomic analysis revealed alterations in proteins related to energy metabolism (Figs 1 and 2) such as reduction in NADH dehydrogenase [ubiquinone] flavoprotein 2, mitochondrial and ATP synthase subunit beta, mitochondrial and increase in D-3-phosphoglycerate dehydrogenase. This has been reported in the liver upon subchronic exposure to F (Pereira et al., 2013; Pereira et al., 2018; Araujo et al., 2019; Trevizol et al., 2020). F is well-known to its ability to inhibit the activity of enolase (Warburg and Christian, 1942). Thus, alterations in proteins involved in energy metabolism may counteract this inhibitory action of F in the activity of enolase, thus maintaining the energy flow (Araujo et al., 2019; Trevizol et al., 2020). Changes in energy metabolism proteins were also reported in the jejunum (Dionizio et al., 2018c).

A decrease in *Gastrotopin* (P80020) was observed in the present study under F exposure, for both doses (Fig.3). This protein, also known as *Fatty acid binding protein 6*, is an important transport protein involved in the enterohepatic circulation of bile salts. It is expressed mainly in the ileum, acts in the absorption of B12 vitamin and binds to bile acids, powerful detergents required for proper digestion and absorption of fats from the diet (Grober et al., 1999; Marvin-Guy et al., 2005; Landrier et al., 2006; Iiizumi et al., 2007; Davis and Attie, 2008; Thompson et al., 2017). The reduction in *Gastrotopin* leads to primary bile acid malabsorption (Balesaria et al., 2008; Keely and Walters, 2016). It is possible that reduction in the expression of bile acids transporters, in the absence of damage, leads to idiopathic bile acid malabsorption, since the absence of expression is involved in malabsorption and diarrhea in cases of ileal resection or inflammatory disease (Jung et al., 2004; Balesaria et al., 2008; Keely and Walters, 2016). Inflammation of the ileum, as occurs in CD or after radiation, provokes bile acid malabsorption and the presence of unabsorbed bile acids in the

colon, leads to diarrhea, by stimulation of fluid and electrolyte secretion, since bile acids have effects on the transport of colonic fluid by indirect and direct actions on the epithelium (Luman et al., 1995; Rossel et al., 1999; Balesaria et al., 2008; Keely and Walters, 2016).

In summary, this study shows that while morphologic changes of the rat ileum due to low (10 mg/L) and high (50 mg/L) F doses were similar, F related effects on the proteome and microbiome differed between the two doses. These results suggest that the effects of F to result inflammatory changes similar to those found in CD, such as an increase in the ileum wall thickness, increase in the SP-IR, CGRP, and VIP-IR varicosities, as well as a decrease in bile acid transporters, such as *Gastrotopin*, may be compounded by additional alterations to the microbiome of the small intestine. The intestinal environment can have profound effects on the activity of the CNS (Houser and Tansey, 2017), and further studies to determine how exposure to low levels of F in drinking water affect the small intestine barrier function and microbiome are needed to understand the potential effects of F ingestion in modulating these functions. Moreover, our results open the avenue for understanding the effects of F on the MGBA, with potential application in the modulation of several diseases in which the gut microbiome is involved.

Supplementary Material

Refer to Web version on PubMed Central for supplementary material.

Acknowledgments

The authors acknowledge helpful discussions with Yukiko Nakano (University of California, San Francisco, USA) and with Gábor Varga (Semmelweis University, Budapest, Hungary), technical assistance of Aline Lima Leite (Bauru Dental School, University of São Paulo, Brazil) and undergraduate students Alessandro Domingues Heube, Juliana Gadelha Souza (Bauru School of Dentistry, University of São Paulo, Brazil) and Sara Raquel Garcia Souza (State University of Maringá, Brazil), for the help with samples collection. This study was supported by FAPESP (2011/10233-7, 2012/16840-5, and 2016/09100-6); T32DE007306 (NIH/NIDCR), and the UCSF Center for Children's Oral Health Research.

REFERENCES

Akiniwa K, 1997. Re-examination of acute toxicity of fluoride. Fluoride 30, 89–104.

Allin KH, Nielsen T, Pedersen O, 2015. Mechanisms in endocrinology: Gut microbiota in patients with type 2 diabetes mellitus. European journal of endocrinology 172, R167–177. [PubMed: 25416725]

Aniwan S, Park SH, Loftus EV Jr., 2017. Epidemiology, Natural History, and Risk Stratification of Crohn's Disease. Gastroenterology clinics of North America 46, 463–480. [PubMed: 28838409]

Araujo TT, Barbosa Silva Pereira HA, Dionizio A, Sanchez CDC, de Souza Carvalho T, da Silva Fernandes M, Rabelo Buzalaf MA, 2019. Changes in energy metabolism induced by fluoride: Insights from inside the mitochondria. Chemosphere 236, 124357. [PubMed: 31325826]

Ardizzone S, Bianchi Porro G, 2002. Inflammatory bowel disease: new insights into pathogenesis and treatment. Journal of internal medicine 252, 475–496. [PubMed: 12472908]

Augenstein WL, Spoerke DG, Kulig KW, Hall AH, Hall PK, Riggs BS, el Saadi M, Rumack BH, 1991. Fluoride ingestion in children: a review of 87 cases. Pediatrics 88, 907–912. [PubMed: 1945630]

Baker JL, Sudarsan N, Weinberg Z, Roth A, Stockbridge RB, Breaker RR, 2012. Widespread genetic switches and toxicity resistance proteins for fluoride. Science 335, 233–235. [PubMed: 22194412]

Balesaria S, Pell RJ, Abbott LJ, Tasleem A, Chavele KM, Barley NF, Khair U, Simon A, Moriarty KJ, Brydon WG, Walters JR, 2008. Exploring possible mechanisms for primary bile acid malabsorption:

evidence for different regulation of ileal bile acid transporter transcripts in chronic diarrhoea. European journal of gastroenterology & hepatology 20, 413–422. [PubMed: 18403943]

Barbier O, Arreola-Mendoza L, Del Razo LM, 2010. Molecular mechanisms of fluoride toxicity. Chem Biol Interact 188, 319–333. [PubMed: 20650267]

Bell JS, Spencer JI, Yates RL, Yee SA, Jacobs BM, DeLuca GC, 2019. Invited Review: From nose to gut - the role of the microbiome in neurological disease. Neuropath Appl Neuro 45, 195–215.

Boyer L, Sidpra D, Jevon G, Buchan AM, Jacobson K, 2007. Differential responses of VIPergic and nitrergic neurons in paediatric patients with Crohn's disease. Autonomic neuroscience : basic & clinical 134, 106–114. [PubMed: 17466601]

Chelakkot C, Ghim J, Ryu SH, 2018. Mechanisms regulating intestinal barrier integrity and its pathological implications. Exp Mol Med 50, 103.

Chiorean L, Schreiber-Dietrich D, Braden B, Cui X, Dietrich CF, 2014. Transabdominal ultrasound for standardized measurement of bowel wall thickness in normal children and those with Crohn's disease. Medical ultrasonography 16, 319–324. [PubMed: 25463885]

Chu J, Pham NT, Olate N, Kislitsyna K, Day MC, LeTourneau PA, Kots A, Stewart RH, Laine GA, Cox CS Jr., Uray K, 2013. Biphasic regulation of myosin light chain phosphorylation by p21-activated kinase modulates intestinal smooth muscle contractility. The Journal of biological chemistry 288, 1200–1213. [PubMed: 23161543]

Collins SM, Bercik P, 2009. The relationship between intestinal microbiota and the central nervous system in normal gastrointestinal function and disease. Gastroenterology 136, 2003–2014. [PubMed: 19457424]

Csordas A, 1996. Butyrate, aspirin and colorectal cancer. Eur J Cancer Prev 5, 221–231. [PubMed: 8894559]

Das TK, Susheela AK, Gupta IP, Dasarathy S, Tandon RK, 1994. Toxic effects of chronic fluoride ingestion on the upper gastrointestinal tract. Journal of clinical gastroenterology 18, 194–199. [PubMed: 8034913]

Davis RA, Attie AD, 2008. Deletion of the ileal basolateral bile acid transporter identifies the cellular sentinels that regulate the bile acid pool. Proceedings of the National Academy of Sciences of the United States of America 105, 4965–4966. [PubMed: 18362334]

Dionizio A, Pereira H, Araujo TT, Sabino-Arias IT, Fernandes MS, Oliveira KA, Raymundo FS, Cestari TM, Nogueira FN, Carvalho RA, Buzalaf MAR, 2018a. Effect of Duration of Exposure to Fluoride and Type of Diet on Lipid Parameters and De Novo Lipogenesis. Biological trace element research 190, 157–171. [PubMed: 30328034]

Dionizio AS, Melo CGS, Sabino-Arias IT, Ventura TMS, Leite AL, Souza SRG, Santos EX, Heubel AD, Souza JG, Perles J, Zanoni JN, Buzalaf MAR, 2018b. Chronic treatment with fluoride affects the jejunum: insights from proteomics and enteric innervation analysis. Scientific reports 8, 3180. [PubMed: 29453425]

Dionizio AS, Melo CGS, Sabino-Arias IT, Ventura TMS, Leite AL, Souza SRG, Santos EX, Heubel AD, Souza JG, Perles J, Zanoni JN, Buzalaf MAR, 2020. Effects of acute fluoride exposure on the jejunum and ileum of rats. Science of the total environment, 1.

Dionizio AS, Melo CGS, Sabino-Arias IT, Ventura TMS, Leite AL, Souza SRG, Santos EX, Heubel AD, Souza JG, Perles J.V.C.M.J.S.r., 2018c. Chronic treatment with fluoride affects the jejunum: insights from proteomics and enteric innervation analysis. 8, 1–12.

Duan Q, Jiao J, Chen X, Wang X, 2018. Association between water fluoride and the level of children's intelligence: a dose-response meta-analysis. Public health 154, 87–97. [PubMed: 29220711]

Dunipace AJ, Kelly SA, Wilson ME, Zhang W, Denzinger S, Brizendine E, 1995. Correlation of Fluoride Levels in Human Plasma, Urine and Saliva. Journal of Dental Research 74, 134–134.

Felice VD, O'Mahony SM, 2017. The microbiome and disorders of the central nervous system. Pharmacol Biochem Be 160, 1–13.

Fond G, Boukouaci W, Chevalier G, Regnault A, Eberl G, Hamdani N, Dickerson F, Macgregor A, Boyer L, Dargel A, Oliveira J, Tamouza R, Leboyer M, 2015. The "psychomicrobiotic": Targeting microbiota in major psychiatric disorders: A systematic review. Pathol Biol 63, 35–42. [PubMed: 25468489]

Furness JB, 2006. A comprehensive overview of all aspects of the enteric nervous system. The enteric nervous system, Oxford.

Gajendran M, Loganathan P, Catinella AP, Hashash JG, 2017. A comprehensive review and update on Crohn's disease. Disease-a-month : DM.

Gessner BD, Beller M, Middaugh JP, Whitford GM, 1994. Acute fluoride poisoning from a public water system. N Engl J Med 330, 95–99. [PubMed: 8259189]

Goschorska M, Gutowska I, Baranowska-Bosiacka I, Piotrowska K, Metryka E, Safranow K, Chlubek D, 2018. Influence of Acetylcholinesterase Inhibitors Used in Alzheimer's Disease Treatment on the Activity of Antioxidant Enzymes and the Concentration of Glutathione in THP-1 Macrophages under Fluoride-Induced Oxidative Stress. Int J Environ Res Public Health 16.

Goto Y, Kurashima Y, Kiyono H, 2015. The gut microbiota and inflammatory bowel disease. Current opinion in rheumatology 27, 388–396. [PubMed: 26002031]

Grober J, Zaghini I, Fujii H, Jones SA, Kliewer SA, Willson TM, Ono T, Besnard P, 1999. Identification of a bile acid-responsive element in the human ileal bile acid-binding protein gene. Involvement of the farnesoid X receptor/9-cis-retinoic acid receptor heterodimer. The Journal of biological chemistry 274, 29749–29754. [PubMed: 10514450]

Guyton AC, Hall JE, 2015. Textbook of medical physiology, 13 ed. Elsevier Health Sciences, Philadelphia.

Holzer P, Lippe IT, 1984. Substance P can contract the longitudinal muscle of the guinea-pig small intestine by releasing intracellular calcium. British journal of pharmacology 82, 259–267. [PubMed: 6203591]

Houser MC, Tansey MG, 2017. The gut-brain axis: is intestinal inflammation a silent driver of Parkinson's disease pathogenesis? NPJ Parkinsons Dis 3, 3. [PubMed: 28649603]

Iheozor-Ejiofor Z, Worthington HV, Walsh T, O'Malley L, Clarkson JE, Macey R, Alam R, Tugwell P, Welch V, Glenny AM, 2015. Water fluoridation for the prevention of dental caries. Cochrane Database Syst Rev, CD010856. [PubMed: 26092033]

Iiizumi G, Sadoya Y, Hino S, Shibuya N, Kawabata H, 2007. Proteomic characterization of the site-dependent functional difference in the rat small intestine. Biochimica et biophysica acta 1774, 1289–1298. [PubMed: 17881305]

Johnson BM, Gaudreau MC, Al-Gadban MM, Gudi R, Vasu C, 2015. Impact of dietary deviation on disease progression and gut microbiome composition in lupus-prone SNF1 mice. Clinical and experimental immunology 181, 323–337. [PubMed: 25703185]

Jung D, Fantin AC, Scheurer U, Fried M, Kullak-Ublick GA, 2004. Human ileal bile acid transporter gene ASBT (SLC10A2) is transactivated by the glucocorticoid receptor. Gut 53, 78–84. [PubMed: 14684580]

Kang B, Choi SY, Chi S, Lim Y, Jeon TY, Choe YH, 2017. Baseline Wall Thickness Is Lower in Mucosa-Healed Segments 1 Year After Infliximab in Pediatric Crohn Disease Patients. Journal of pediatric gastroenterology and nutrition 64, 279–285. [PubMed: 27050057]

Kastl AJ Jr., Terry NA, Wu GD, Albenberg LG, 2020. The Structure and Function of the Human Small Intestinal Microbiota: Current Understanding and Future Directions. Cellular and molecular gastroenterology and hepatology 9, 33–45. [PubMed: 31344510]

Keely SJ, Walters JR, 2016. The Farnesoid X Receptor: Good for BAD. Cellular and molecular gastroenterology and hepatology 2, 725–732. [PubMed: 28174746]

Landrier JF, Eloranta JJ, Vavricka SR, Kullak-Ublick GA, 2006. The nuclear receptor for bile acids, FXR, transactivates human organic solute transporter-alpha and -beta genes. American journal of physiology. Gastrointestinal and liver physiology 290, G476–485. [PubMed: 16269519]

Laserna-Mendieta EJ, Clooney AG, Carretero-Gomez JF, Moran C, Sheehan D, Nolan JA, Hill C, Gahan CGM, Joyce SA, Shanahan F, Claesson MJ, 2018. Determinants of Reduced Genetic Capacity for Butyrate Synthesis by the Gut Microbiome in Crohn's Disease and Ulcerative Colitis. J Crohns Colitis 12, 204–216. [PubMed: 29373727]

Lee SH, 2015. Intestinal permeability regulation by tight junction: implication on inflammatory bowel diseases. Intest Res 13, 11–18. [PubMed: 25691839]

Lembeck F, 1988. The 1988 Ulf Euler Lecture. Substancce P: from extract to excitement. Acta physiologica Scandinavica 133, 435–454. [PubMed: 2465671]

Lerner A, Matthias T, 2015. Rheumatoid arthritis-celiac disease relationship: joints get that gut feeling. Autoimmunity reviews 14, 1038–1047. [PubMed: 26190704]

Lima Leite A, Gualiume Vaz Madureira Lobo J, Barbosa da Silva Pereira HA, Silva Fernandes M, Martini T, Zucki F, Sumida DH, Rigalli A, Buzalaf MA, 2014. Proteomic analysis of gastrocnemius muscle in rats with streptozotocin-induced diabetes and chronically exposed to fluoride. PLoS One 9, e106646. [PubMed: 25180703]

Liu T, Zhang L, Joo D, Sun SC, 2017. NF-kappaB signaling in inflammation. Signal Transduct Target Ther 2.

Llorente C, Schnabl B, 2015. The gut microbiota and liver disease. Cellular and molecular gastroenterology and hepatology 1, 275–284. [PubMed: 26090511]

Luhrs H, Gerke T, Schauber J, Dusel G, Melcher R, Scheppach W, Menzel T, 2001. Cytokine-activated degradation of inhibitory kappaB protein alpha is inhibited by the shortchain fatty acid butyrate. Int J Colorectal Dis 16, 195–201. [PubMed: 11515677]

Luman W, Williams AJ, Merrick MV, Eastwood MA, 1995. Idiopathic bile acid malabsorption: long-term outcome. European journal of gastroenterology & hepatology 7, 641–645. [PubMed: 8590159]

Makharia GK, 2011. Understanding and treating abdominal pain and spasms in organic gastrointestinal diseases: inflammatory bowel disease and biliary diseases. Journal of clinical gastroenterology 45 Suppl, S89–93. [PubMed: 21666426]

Mantyh CR, Vigna SR, Bollinger RR, Mantyh PW, Maggio JE, Pappas TN, 1995. Differential expression of substance P receptors in patients with Crohn's disease and ulcerative colitis. Gastroenterology 109, 850–860. [PubMed: 7657114]

Mantyh PW, 1991. Substance P and the inflammatory and immune response. Annals of the New York Academy of Sciences 632, 263–271. [PubMed: 1719871]

Marvin-Guy L, Lopes LV, Affolter M, Courtet-Compondu MC, Wagniere S, Bergonzelli GE, Fay LB, Kussmann M, 2005. Proteomics of the rat gut: analysis of the myenteric plexus-longitudinal muscle preparation. Proteomics 5, 2561–2569. [PubMed: 15984044]

Mazumdar S, Das KM, 1992. Immunocytochemical localization of vasoactive intestinal peptide and substance P in the colon from normal subjects and patients with inflammatory bowel disease. The American journal of gastroenterology 87, 176–181. [PubMed: 1370872]

McCoy KD, Koller Y, 2015. New developments providing mechanistic insight into the impact of the microbiota on allergic disease. Clinical immunology 159, 170–176. [PubMed: 25988860]

Melo CGS, Perles J, Zanoni JN, Souza SRG, Santos EX, Leite AL, Heubel AD, CO ES, Souza JG, Buzalaf MAR, 2017. Enteric innervation combined with proteomics for the evaluation of the effects of chronic fluoride exposure on the duodenum of rats. Scientific reports 7, 1070. [PubMed: 28432311]

Munster T, Eckl S, Leis S, Gohring-Waldeck G, Ihmsen H, Maihofner C, 2015. Characterization of Somatosensory Profiles in Patients with Crohn's Disease. Pain Pract 15, 265–271. [PubMed: 25597809]

Nopakun J, Messer HH, 1990. Mechanism of fluoride absorption from the rat small intestine. Nutr Res 10, 771–779.

Nopakun J, Messer HH, Voller V, 1989. Fluoride absorption from the gastrointestinal tract of rats. J Nutr 119, 1411–1417. [PubMed: 2585131]

Ooi CJ, Makharia GK, Hilmi I, Gibson PR, Fock KM, Ahuja V, Ling KL, Lim WC, Thia KT, Wei SC, Leung WK, Koh PK, Gearry RB, Goh KL, Ouyang Q, Sollano J, Manatsathit S, de Silva HJ, Rerknimitr R, Pisespongsa P, Abu Hassan MR, Sung J, Hibi T, Boey CC, Moran N, Leong RW, Asia Pacific Association of Gastroenterology Working Group on Inflammatory Bowel D, 2016. Asia-Pacific consensus statements on Crohn's disease. Part 2: Management. Journal of gastroenterology and hepatology 31, 56–68. [PubMed: 25819311]

Pereira H, Dionizio AS, Araujo TT, Fernandes MDS, Iano FG, Buzalaf MAR, 2018. Proposed mechanism for understanding the dose- and time-dependency of the effects of fluoride in the liver. Toxicology and applied pharmacology 358, 68–75. [PubMed: 30217653]

Pereira HA, Leite Ade L, Charone S, Lobo JG, Cestari TM, Peres-Buzalaf C, Buzalaf MA, 2013. Proteomic analysis of liver in rats chronically exposed to fluoride. PLoS One 8, e75343. [PubMed: 24069403]

Pryde SE, Duncan SH, Hold GL, Stewart CS, Flint HJ, 2002. The microbiology of butyrate formation in the human colon. FEMS Microbiol Lett 217, 133–139. [PubMed: 12480096]

Racz R, Foldes A, Bori E, Zsembery A, Harada H, Steward MC, DenBesten P, Bronckers A, Gerber G, Varga G, 2017. No Change in Bicarbonate Transport but Tight-Junction Formation Is Delayed by Fluoride in a Novel Ameloblast Model. Front Physiol 8, 940. [PubMed: 29375389]

Rosenbaum DG, Conrad MA, Biko DM, Ruchelli ED, Kelsen JR, Anupindi SA, 2017. Ultrasound and MRI predictors of surgical bowel resection in pediatric Crohn disease. Pediatric radiology 47, 55–64. [PubMed: 27687769]

Rossel P, Sortsoe Jensen H, Qvist P, Arveschoug A, 1999. Prognosis of adult-onset idiopathic bile acid malabsorption. Scandinavian journal of gastroenterology 34, 587–590. [PubMed: 10440608]

Sand E, Roth B, Westrom B, Bonn P, Ekblad E, Ohlsson B, 2014. Structural and functional consequences of buserelin-induced enteric neuropathy in rat. BMC gastroenterology 14, 209. [PubMed: 25496312]

Segain JP, Raingeard de la Bletiere D, Bourreille A, Leray V, Gervois N, Rosales C, Ferrier L, Bonnet C, Blottiere HM, Galmiche JP, 2000. Butyrate inhibits inflammatory responses through NFkappaB inhibition: implications for Crohn's disease. Gut 47, 397–403. [PubMed: 10940278]

Sender R, Fuchs S, Milo R, 2016. Revised Estimates for the Number of Human and Bacteria Cells in the Body. PLoS biology 14, e1002533. [PubMed: 27541692]

Sharma JD, Jain P & Sohu D, 2009. Gastric Discomforts from Fluoride in Drinking Water in Sanganer Tehsil, Rajasthan, India. Fluoride 42, 286–291

Shen L, Black ED, Witkowski ED, Lencer WI, Guerriero V, Schneeberger EE, Turner JR, 2006. Myosin light chain phosphorylation regulates barrier function by remodeling tight junction structure. J Cell Sci 119, 2095–2106. [PubMed: 16638813]

Soares A, Beraldi EJ, Ferreira PE, Bazotte RB, Buttow NC, 2015. Intestinal and neuronal myenteric adaptations in the small intestine induced by a high-fat diet in mice. BMC gastroenterology 15, 3. [PubMed: 25609418]

Soderholm JD, Olaison G, Peterson KH, Franzen LE, Lindmark T, Wiren M, Tagesson C, Sjodahl R, 2002. Augmented increase in tight junction permeability by luminal stimuli in the non-inflamed ileum of Crohn's disease. Gut 50, 307–313. [PubMed: 11839706]

Spak CJ, Sjostedt S, Eleborg L, Veress B, Perbeck L, Ekstrand J, 1990. Studies of human gastric mucosa after application of 0.42% fluoride gel. J Dent Res 69, 426–429. [PubMed: 2307744]

Strunecka A, Patocka J, Blaylock R, Chinoy N, 2007. Fluoride interactions: from molecules to disease. Current Signal Transduction Therapy 2, 190–213.

Strunecka A, Strunecky O, 2019. Chronic Fluoride Exposure and the Risk of Autism Spectrum Disorder. Int J Environ Res Public Health 16.

Susheela A, Kumar A, Bhatnagar M, Bahadur R, 1993. Prevalence of endemic Fluorosis with gastrointestinal manifestations in People living in some North-Indian villages. Fluoride 26, 97–104.

Susheela A.e.a., 1992. Fluoride ingestion and its correlation with gastrointestinal discomfort Fluoride 25, 5–22.

Tai N, Wong FS, Wen L, 2015. The role of gut microbiota in the development of type 1, type 2 diabetes mellitus and obesity. Reviews in endocrine & metabolic disorders 16, 55–65. [PubMed: 25619480]

Tavano F, di Mola FF, Latiano A, Palmieri O, Bossa F, Valvano MR, Latiano T, Annese V, Andriulli A, di Sebastiano P, 2012. Neuroimmune interactions in patients with inflammatory bowel diseases: disease activity and clinical behavior based on Substance P serum levels. J Crohns Colitis 6, 563–570. [PubMed: 22398048]

ten Cate JM, Buzalaf MAR, 2019. Fluoride Mode of Action: Once There Was an Observant Dentist.Journal of Dental Research 98, 725–730. [PubMed: 31219410]

Thompson CA, Wojta K, Pulakanti K, Rao S, Dawson P, Battle MA, 2017. GATA4 Is Sufficient to Establish Jejunal Versus Ileal Identity in the Small Intestine. Cellular and molecular gastroenterology and hepatology 3, 422–446. [PubMed: 28462382]

Trevizol JS, Buzalaf NR, Dionizio A, Delgado AQ, Cestari TM, Bosqueiro JR, Magalhaes AC, Buzalaf MAR, 2020. Effects of low-level fluoride exposure on glucose homeostasis in female NOD mice. Chemosphere 254, 126602. [PubMed: 32334241]

Vogt RL, Witherell L, LaRue D, Klaucke DN, 1982. Acute fluoride poisoning associated with an on-site fluoridator in a Vermont elementary school. Am J Public Health 72, 1168–1169. [PubMed: 7114344]

Warburg O, Christian W, 1942. Insulation and crystalisation of the fermenting process of Enolase. Biochem Z 310, 384–421.

Waugh DT, 2019. The Contribution of Fluoride to the Pathogenesis of Eye Diseases: Molecular Mechanisms and Implications for Public Health. Int J Environ Res Public Health 16.

Wei Q, Deng H, Cui H, Fang J, Zuo Z, Deng J, Li Y, Wang X, Zhao L, 2018. A mini review of fluoride-induced apoptotic pathways. Environ Sci Pollut Res Int 25, 33926–33935. [PubMed: 30338467]

Whitford GM, Pashley DH, 1984. Fluoride absorption: the influence of gastric acidity. Calcif Tissue Int 36, 302–307. [PubMed: 6088010]

Worlicek H, Lutz H, Heyder N, Matek W, 1987. Ultrasound findings in Crohn's disease and ulcerative colitis: a prospective study. Journal of clinical ultrasound : JCU 15, 153–163. [PubMed: 3134409]

Wright EK, Kamm MA, Teo SM, Inouye M, Wagner J, Kirkwood CD, 2015. Recent advances in characterizing the gastrointestinal microbiome in Crohn's disease: a systematic review. Inflammatory bowel diseases 21, 1219–1228. [PubMed: 25844959]

Yan YX, Gong YW, Guo Y, Lv Q, Guo C, Zhuang Y, Zhang Y, Li R, Zhang XZ, 2012. Mechanical strain regulates osteoblast proliferation through integrin-mediated ERK activation. PLoS One 7, e35709. [PubMed: 22539993]

Yasuda K, Hsu T, Gallini CA, Mclver LJ, Schwager E, Shi A, DuLong CR, Schwager RN, Abu-Ali GS, Franzosa EA, Garrett WS, Huttenhower C, Morgan XC, 2017. Fluoride Depletes Acidogenic Taxa in Oral but Not Gut Microbial Communities in Mice. Msystems 2.

Zheng Y, Wu J, Ng JC, Wang G, Lian W, 2002. The absorption and excretion of fluoride and arsenic in humans. Toxicol Lett 133, 77–82. [PubMed: 12076512]

Zuo H, Chen L, Kong M, Qiu LP, Lu P, Wu P, Yang YH, Chen KP, 2018. Toxic effects of fluoride on organisms. Life Sci 198, 18–24. [PubMed: 29432760]

Highlights

- Fluoridated water increases the thickness of the ileum wall;
- Fluoridated water increases CGRP-IR and SP-IR varicosities in the ileum;
- Proteomic changes induced by fluoride have similarity with Crohn's disease;
- Microbiomic changes induced by fluoride are associated with inflammation.

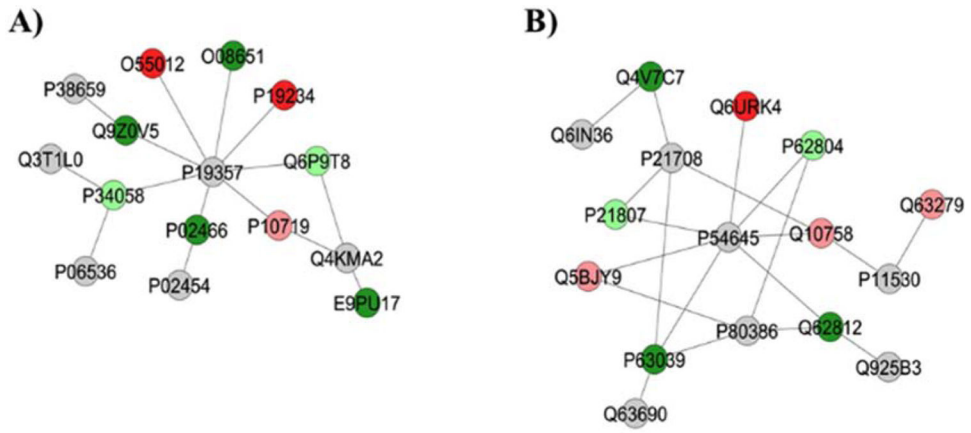

Figure 1 –.

Subnetworks generated by ClusterMarker® for the comparison 10 mgF/L vs. Control (deionized water). The colors of the nodes indicate the differential expression of the respective protein with its access code, available from UniProt protein database (http://www.uniprot.org/). The dark green and dark red nodes indicate proteins unique to 10 mgF/L and Control groups, respectively. The light red and light green nodes indicate down and upregulated proteins, respectively, in 10 mgF/L group in respect to Control. The gray nodes indicate the interaction proteins that are offered by CYTOSCAPE®, which were not identified in the present study.

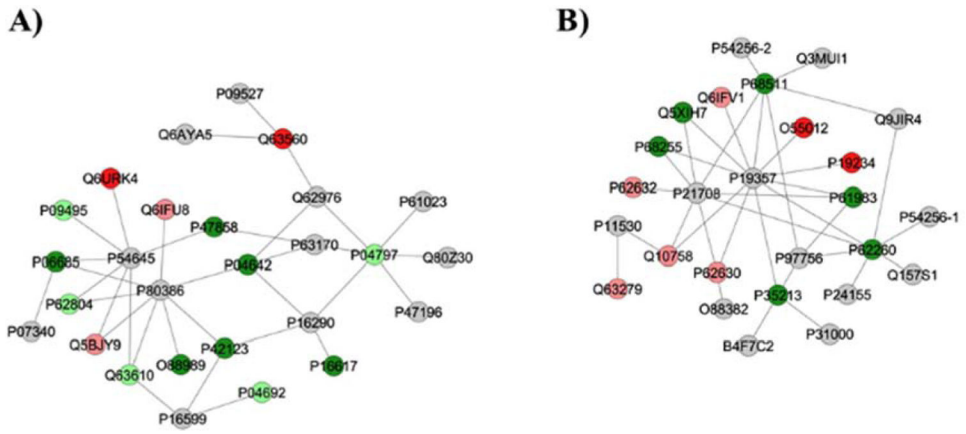

Figure 2 –.

Subnetworks generated by ClusterMarker® for the comparison 50 mgF/L vs. Control (deionized water). The colors of the nodes indicate the differential expression of the respective protein with its access code, available from UniProt protein database (http://www.uniprot.org/). The dark green and dark red nodes indicate proteins unique to 50 mgF/L and Control groups, respectively. The light red and light green nodes indicate down and upregulated proteins, respectively, in 50 mgF/L group in respect to Control. The gray nodes indicate the interaction proteins that are offered by CYTOSCAPE®, which were not identified in the present study.

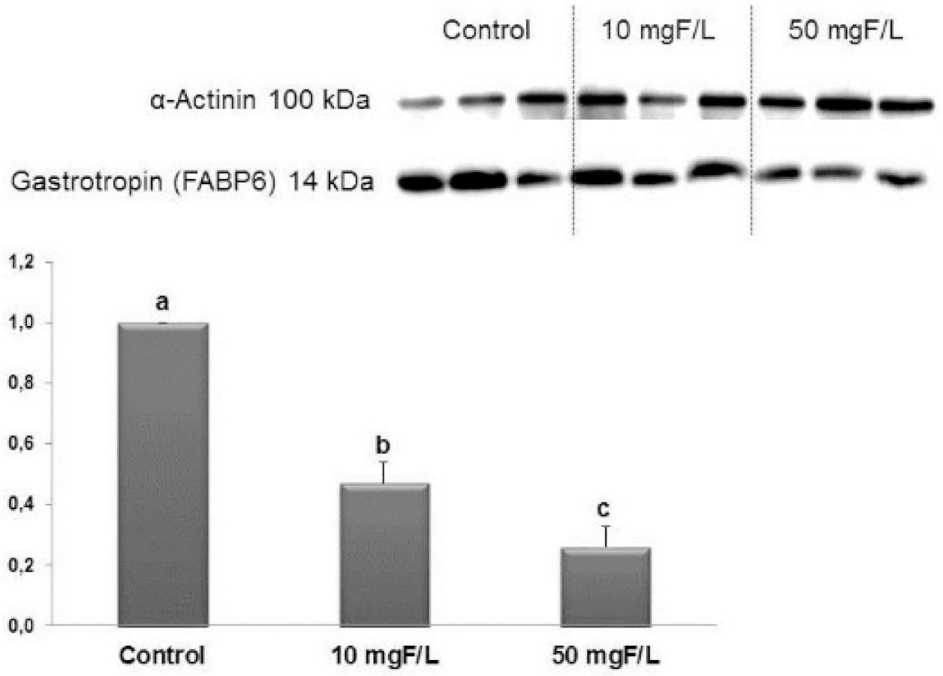

Figure 3–.

Representative expression of proteins *Gastrotropin* and of the constitutive protein α-Actinin in samples of individual animals (n = 6) from each group. Densitometric analysis was performed for 6 animals per group. Densitometry was analyzed using the software Image Studio Lite. Distinct letters denote significant differences among the groups (ANOVA and Tukey's test, $p<0.05$). Bars indicate SD. n = 6

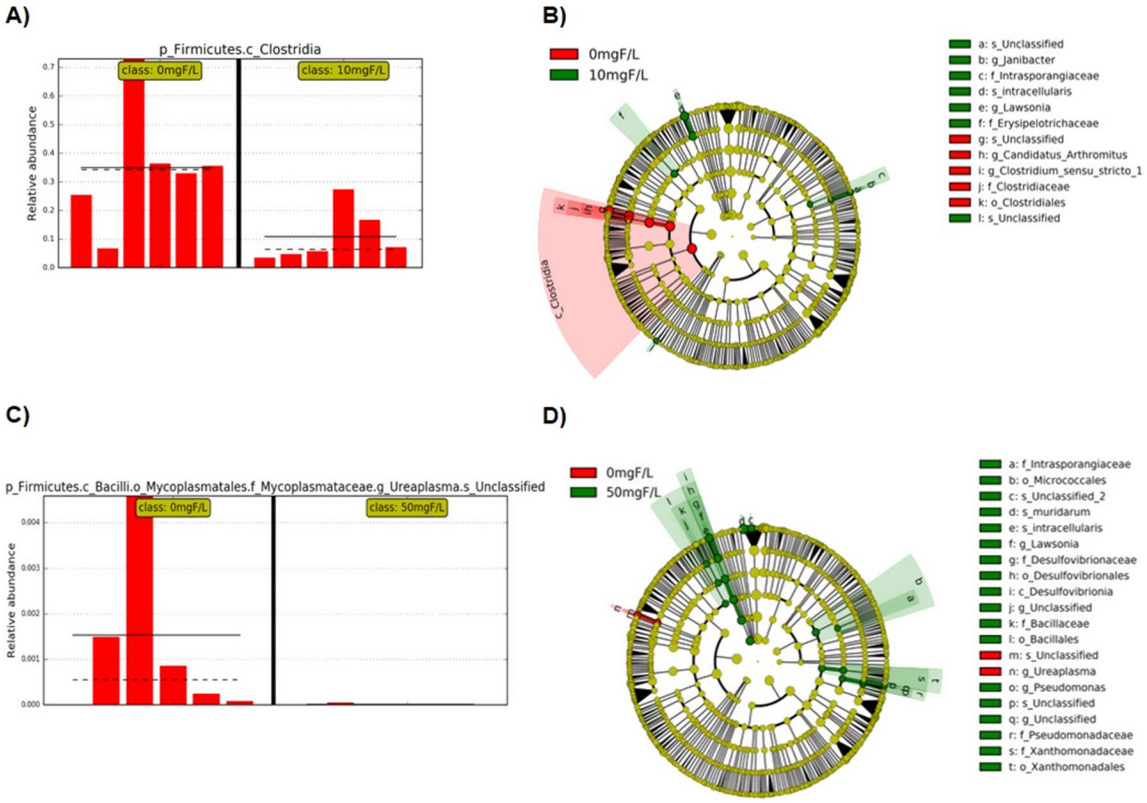

Figure 4–.

Bar plots and cladograms showing the differentially expressed taxa; **A)** Bar plot showing the relative abundance of class clostridia when control and 10 mgF/L groups were compared, each group means represented with straight line and the medians represented with dotted line; **B)** Cladogram (result from LEfSe analysis) of significantly different taxa (highlighted by small circles and by shading) when compared control to 10 mgF/L. Differences are represented in the color of the most abundant class (red indicating 0 mgF/L group, green indicating 10mgF/L and yellow non-significant). Each circle's diameter is proportional to the taxon's abundance; **C)** Bar plot showing the relative abundance of unclassified species in genus Ureaplasma when control and 50 mgF/L groups were compared; **D)** Cladogram of significantly different taxa when compared the control and 50 mgF/L groups.

Table 1.

Means and standard deviations of the values of the cell bodies areas and density of HUC/D-IR and nNOS-IR neurons and VIP-IR, CGRP-IR, and SP-IR values of myenteric neurons varicosities areas of the ileum of rats subchronically exposed, or not exposed, to fluoride in the drinking water.

ANALYSIS	Control	10 mgF/L	50 mgF/L
Cell bodies areas of the HuC/D-IR neurons (μm^2)	315.1±4.0[a]	311.8±3.9[a]	321.6±3.6[a]
Density HuC/D-IR neurons (neurons/cm^2)	16.626,7±493.6[a]	14.990,2±419.1[b]	14.615,6±461.9[b]
Cell bodies areas of the nNOS-IR neurons (μm^2)	293.1±3.1[a]	300.0±3.4[a]	290.2±3.2[a]
Density nNOS-IR neurons (neurons/cm^2)	4.563,4±130.5[a]	4.334,9±119.6[a]	4.353,9±136.1[a]
Area VIP-IR varicosities (μm^2)	3.55±0.03[a]	3.55±0.04[a]	4.67±0.05[b]
Area CGRP-IR varicosities (μm^2)	3.24±0.02[a]	3.42±0.03[b]	3.58±0.03[c]
Area SP-IR varicosities (μm^2)	2.89±0.02[a]	4.58±0.02[b]	4.64±0.03[b]

Means followed by distinct letters in the same line are significantly different according to ANOVA followed by Fisher's test (density HuC/D-IR and nNOS-IR neurons) or ANOVA followed by Tukey's test (other variables). $p < 0.05$. $n = 6$.

Table 2.

Most abundant phylum, Class, Family, and Genus in the ileum of rats.

At Phylum level	At Class level	At the Family level	At the Genus level
Campilobacterota (67.8%)	Campylobacteria (67.9%)	Helicobacteraceae (65.5%)	Helicobacter (64.6%),
Firmicutes (24.4%)	Clostridia (22.4%)	Clostridiaceae (20.4%)	Candidatus_Arthromitus (20.2%)
Proteobacteria (6.2%)	Gammaproteobacteria (6.2%)	Enterobacteriacease (4.4%)	Escherichia/Shigella (4.4%)
Desulfobacterota (1.6%)	Bacilli (1.8%)	Campylobacteracease (3.5%)	Campylobacter (3.5%)